Volume 6 | Number 3 | 7 February 2014 | Pages 1211–1902

Nanoscale

www.rsc.org/nanoscale

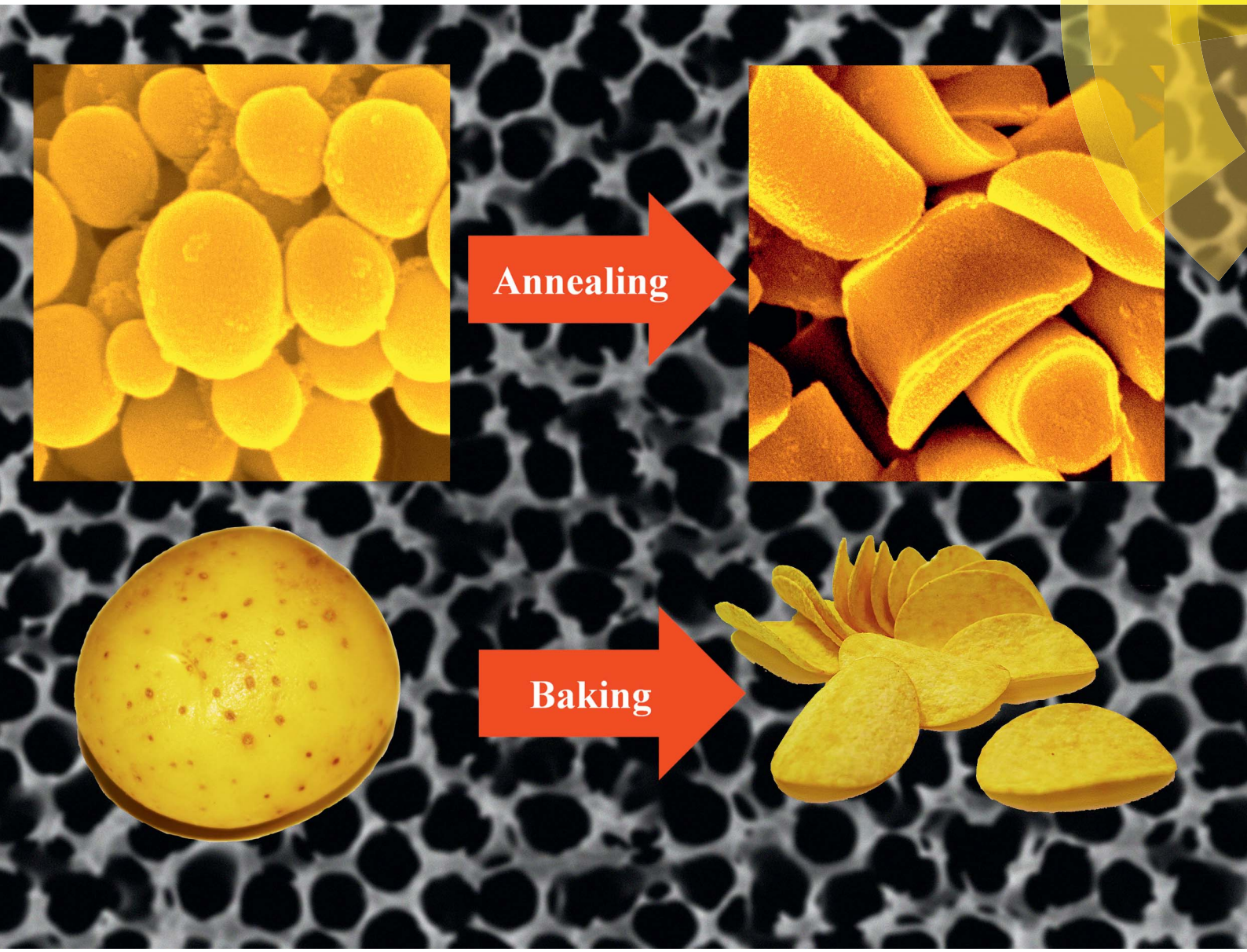

ISSN 2040-3364

ROYAL SOCIETY OF CHEMISTRY

PAPER
Chen *et al.*
Curved polymer nanodiscs by wetting nanopores of anodic aluminum oxide templates with polymer nanospheres

NCNST

Nanoscale

PAPER

View Article Online
View Journal | View Issue

Cite this: *Nanoscale*, 2014, **6**, 1340

Curved polymer nanodiscs by wetting nanopores of anodic aluminum oxide templates with polymer nanospheres†

Mu-Huan Chi, Yi-Huei Kao, Tzu-Hui Wei, Chih-Wei Lee and Jiun-Tai Chen*

Received 20th August 2013
Accepted 12th November 2013

DOI: 10.1039/c3nr04431a

www.rsc.org/nanoscale

Although nanostructures with diverse morphologies have been fabricated, it is still a great challenge to prepare anisotropic two-dimensional (2-D) nanostructures, especially non-planar disc-like nanostructures. In this work, we develop a simple method to prepare curved polymer nanodiscs with regular sizes by wetting polymer nanospheres in the nanopores of anodic aluminum oxide (AAO) templates. Polystyrene (PS) nanospheres are first fabricated by using a non-solvent-assisted template wetting method. By annealing the PS nanospheres in the nanopores of AAO templates, curved PS nanodiscs can be produced. The length and morphology of the curved PS nanodiscs can be controlled by the wetting conditions such as the annealing temperatures and times. For some stacked nanospheres, the annealing process can result in the formation of helix-like nanostructures. To demonstrate the universality of this work, this approach is also applied to poly(methyl methacrylate) (PMMA), another common polymer, and similar results are obtained.

Introduction

In the past two decades, nanomaterials have received much attention because of their unique properties, which are different from those in the bulk state.[1] Different methods have been developed to prepare zero-dimensional (0-D) or one-dimensional (1-D) nanostructures.[2–5] These nanostructures have been studied intensively and are applied in many different fields such as photoelectric devices, microfluidics, catalysts, separation membranes, sensors, or drug delivery.[6–11] Recently, two-dimensional (2-D) nanostructures have also attracted great interest and can be produced by different methods. 2-D nanomaterials such as graphene nanoplates, zinc oxide (ZnO) discs, or silver discs are prepared and can be applied in photoelectric devices, sensors, flat panels, and purification.[12–16] While most studies on 2-D nanostructures focus on metals or inorganic materials, organic or polymer based 2-D nanostructures are less studied.

In 1993, Ho *et al.* developed a stretching method, which can be used to prepare anisotropic 2-D polymer microstructures with regular sizes.[17] In 2006, Champion *et al.* modified this method to prepare polymer microdiscs.[18] Other groups continually optimized this method to fabricate anisotropic 2-D polymer structures, but most structures prepared by this method are still on the micron scale.[19] In 2012, Liu *et al.* also successfully fabricated polymer nanodiscs from nanospheres by stirring polymer nanospheres in mixed solvents.[20] Despite these works, it is still a great challenge to prepare anisotropic two-dimensional (2-D) nanostructures, especially non-planar disc-like nanostructures. Here, we develop a simple template-based wetting method to prepare curved polymer nanodiscs by wetting polymer nanospheres in the nanopores of anodic aluminum oxide (AAO) templates.

The template-based wetting method has been widely used to prepare polymer nanomaterials with different geometries.[21–24] Polymer solutions or melts are introduced to the nanopores of the porous templates by wetting.[25] After the solidification of the polymers in the nanopores, polymer nanostructures can be formed after the porous templates are selectively removed. One of the main advantages of using the template method is that the sizes of the prepared nanostructures can be controlled by the pore sizes of the porous templates. Various polymer nanostructures have been prepared in the past, and properties and morphologies, which are not present in the bulk, are observed.[26,27] Different polymer nanostructures such as nanotubes, nanorods, nanowires, and nanospheres have been fabricated by the template wetting method.[28–32]

Porous AAO membranes are commonly used as templates for fabricating various metal, inorganic, and polymer nanomaterials.[33] AAO templates are made by the electrochemical oxidation of aluminum foils, and hexagonally packed nanopores can be prepared by using a two-step anodization process.[34] The interpore distances, pore diameters, and thicknesses of the AAO templates can be changed by the anodization

Department of Applied Chemistry, National Chiao Tung University, Hsinchu, Taiwan 30050. E-mail: jtchen@mail.nctu.edu.tw

† Electronic supplementary information (ESI) available: SEM images of AAO templates and polymer nanostructures, and OM images of deposited polymer particles. See DOI: 10.1039/c3nr04431a

conditions such as the anodization voltage, the working temperature, the anodization time, the electrolyte concentration, and the electrolyte solution type.[35]

In this work, we successfully prepared anisotropic, curved polymer nanodiscs by wetting polymer nanospheres in the nanopores of AAO templates. PS nanospheres are first prepared by the non-solvent-assisted template wetting method, which was recently developed by Lee *et al.*[29] After thermal annealing, wetting of the PS nanospheres in the nanopores of AAO templates occurs, resulting in the formation of curved PS nanodiscs. By changing the pore sizes of the AAO template or the conditions of thermal annealing, the morphologies of the PS nanodiscs can be controlled. In addition to PS, poly(methyl methacrylate) (PMMA) is also used. This study not only provides a simple method to fabricate curved polymer nanodiscs, but also leads to a deeper understanding of the wetting phenomenon in confined geometries.

Results and discussion

The concept of fabricating the curved polymer nanodiscs is mainly based on the idea of annealing polymer nanospheres in the nanopores of porous templates. The templates we use are the AAO templates, as shown in the SEM images (Fig. S1a and b†). The average pore diameter is ~230 nm, and the average pore length is ~60 μm. The experimental scheme and the schematic illustration of the formation of curved polymer nanodiscs are shown in Fig. 1 and 2, respectively. At first, PS nanospheres in the nanopores of AAO templates are prepared by the non-solvent-assisted template wetting method, which was developed by Lee *et al.*[29] Normally, polymer nanotubes are produced in the nanopores of AAO templates when a polymer solution is used to wet the nanopores. The formation of nanotubes is caused by the precipitation of the polymer chains on the walls of the AAO templates after the solvents are evaporated. By adding a non-solvent such as water after the nanopores are filled by a polymer solution, water forms wetting layers on the walls of the AAO templates, resulting in the formation of nanospheres or nanorods instead of nanotubes.[29] The formation of nanospheres or nanorods is determined by the polymer concentrations. Lee *et al.* also demonstrated that the aspect ratio (length divided by the diameter) of the polymer nanorods increased with the polymer concentration.[29] For our study here, polymer concentrations in the range of 1.5 to 3 wt% are used, in which polymer nanospheres can be generated.

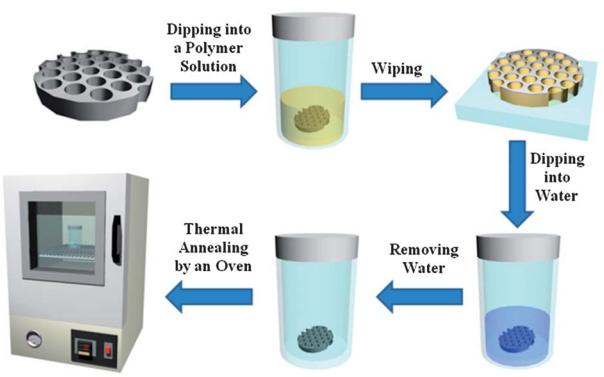

Fig. 1 Experimental scheme to prepare curved polymer nanodiscs.

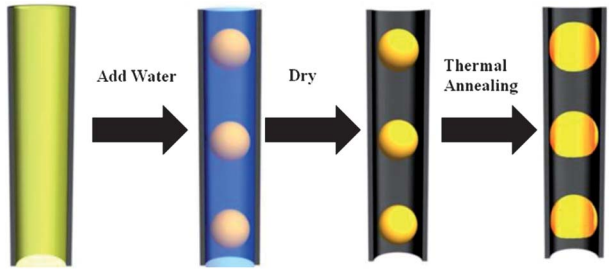

Fig. 2 Schematic illustration of the formation of curved polymer nanodiscs in the nanopores of AAO templates.

After the solvent is evaporated by a vacuum system, polymer nanospheres are formed. The AAO templates containing PS nanospheres are annealed in an oven with different annealing temperatures and times. When the annealing temperatures are above the glass transition temperature of PS (~100 °C), the PS nanospheres can wet the pore walls of the AAO template to reduce the surface energy. Finally, curved PS nanodiscs are formed.

The polymer nanostructures at different stages are examined by both SEM and TEM. Fig. 3a shows the PS nanospheres prepared by using the non-solvent-assisted template wetting method. The AAO templates are dissolved by a $NaOH_{(aq.)}$ solution, and the nanospheres aggregate together. The SEM image shows that almost all PS nanospheres are in a spherical shape,

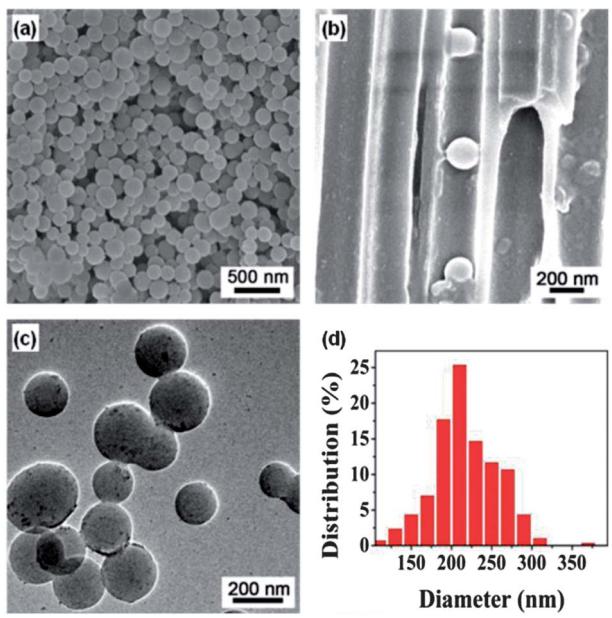

Fig. 3 PS (M_w = 78.5 kg mol^{-1}) nanospheres by using the non-solvent-assisted template wetting method with a PS solution (1.5 wt%): (a) SEM image; (b) cross-sectional SEM image; (c) TEM image; (d) plot of the size distribution of the PS nanospheres.

even though some nanostructures are in a elliptical shape. To check the locations and the sizes of the nanospheres inside the nanopores, cross-sectional SEM images in which the AAO templates are still present are taken, as shown in Fig. 3b. The cross-sectional samples are prepared by breaking AAO template containing PS nanospheres. Although some nanospheres have already fallen out of the nanopores during the preparation of the cross-sectional samples, some other nanospheres are still attached to the walls of the nanopores. The nanospheres are separated from each other in the nanopores, and the distances between adjacent nanospheres are mainly determined by Rayleigh instability.[29] For most nanospheres, the separation of the nanospheres can ensure that the wetting of a nanosphere on the pore wall of the AAO template is not affected by the wetting of other nanospheres. For some nanospheres, which are in contact or close to other nanospheres, interesting morphologies can be formed after the thermal annealing process, which will be demonstrated later in this work. To confirm the solid nature of the nanospheres, TEM is also performed, as shown in Fig. 3c. The sizes of the nanospheres from the TEM image agree well with those from the SEM images. The sizes of individual nanospheres are measured, and the size distribution of the nanospheres prepared by using 1.5 wt% PS (M_w = 78.5 kg mol^{-1}) solution is displayed in Fig. 3d. The average diameter of these PS nanospheres is ~240 nm, which is close to the average pore size of the AAO template (~230 nm). The size distribution of the nanospheres is attributed to the distribution of the pore size of the AAO template and the non-uniform polymer concentrations in the nanopores.

Nichols and Mullins have studied the Rayleigh-instability-type transformation for solid cylinders.[36] They found that the perturbation on the cylinder surface with the maximum growth rate has a wavelength $\lambda_m = 2\pi\sqrt{2}R_0 = 8.89R_0$, where R_0 is the initial radius of the cylinder. The radius of the transformed nanosphere can be obtained as $r = 1.88R_0$. Since the average diameter of the PS nanospheres is measured to be ~240 nm, the undulation wavelength, which is equal to the interspacing between the nanospheres, can be calculated to be ~570 nm. The interspacing between nanospheres can be simply increased by using AAO templates with larger pore diameters.

After the samples are thermally annealed at 130 °C for 30 min, AAO templates are selectively removed by $NaOH_{(aq.)}$, and curved PS nanodiscs are obtained, as shown in Fig. 4a. The shapes of the curved PS nanodiscs are similar to those of commercial potato chips. Wetting of the polymer nanospheres in the cylindrical nanopores occurs during the thermal annealing process. When the annealing temperature is higher than the glass transition temperature of PS, the nanospheres within AAO nanopores can have enough mobilities to wet the wall surface of the AAO nanopores, which possess high surface energies.[37] Similar to the situation of a snow ball melting inside a water pipe, the PS nanospheres wet the curved walls and spread out in all directions. From the SEM (Fig. 4b) and TEM (Fig. 4d) images with higher magnifications, we can confirm that the thicknesses throughout the curved PS nanodiscs are almost the same, implying that the PS chains wet the curved wall uniformly.

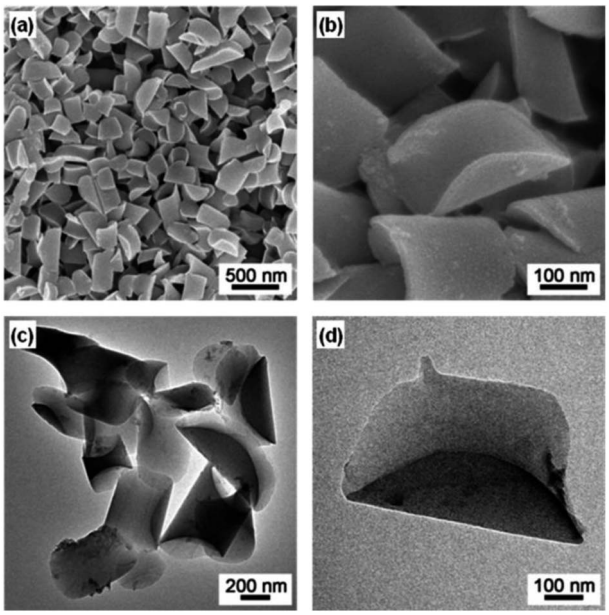

Fig. 4 Curved PS (M_w = 78.5 kg mol^{-1}) nanodiscs by thermally annealing PS nanospheres in the nanopores of AAO templates: (a and b) SEM images; (c and d) TEM images with different magnifications. The PS nanospheres are first prepared by the non-solvent-assisted template wetting method with a PS solution (1.5 wt%), followed by an annealing process at 130 °C for 30 min.

To quantitatively compare the wetting of the PS nanospheres in different conditions, the axis of the nanostructures along the cylindrical nanopores is defined as the *z*-axis. Since the wetting length along the peripheral direction is difficult to be measured from the electron microscopy images, we only measure the wetting lengths along the *z*-axis direction under different annealing conditions. By assuming that the wetting rates of the PS chains in different directions are the same and the gravity effect can be ignored, we presume that the wetting lengths along the peripheral direction are similar to the wetting lengths along the *z*-axis, even though polymers may actually have a preferential wetting direction along the *z*-axis direction. For example, when the polymer chains wet half of the perimeter of the wall surface of the nanopores, the wetting length along the peripheral direction is $(1/2)\pi D_0$, where D_0 is the average diameter of the AAO nanopores (~230 nm). Therefore, the wetting length along the peripheral direction can be calculated to be 361 nm, which is also the wetting length along the *z*-axis. For the curved PS nanodiscs shown in Fig. 4a, which are annealed at 130 °C for 30 min, the average wetting length along the *z*-axis is ~433 nm with the standard deviation of 117 nm. The distribution of the wetting length along the *z*-axis is because of the diameter distribution of the PS nanospheres and the pore size distribution of the AAO template.

We also find that the wetting length of the polymer nanospheres can be affected by the annealing temperature and the annealing time. Fig. S2† shows the SEM images of PS (M_w = 78.5 kg mol^{-1}) nanostructures by annealing PS nanospheres at different temperatures (150, 170, 190, and 210 °C) for 30 min. At high annealing temperatures, the PS melts wet more the pore

walls of the AAO templates, and the wetting lengths along the *z*-axis direction are longer. More irregular edges of the curved PS nanodiscs, however, are generated because more defects on the pore walls are encountered by the front of the wetting polymer melts. Fig. S3† shows the SEM images of PS (M_w = 78.5 kg mol^{-1}) nanostructures by annealing PS nanospheres at 130 °C for different times (20 min, 40 min, 1 h and 2 h). At longer annealing times, the PS melts wet more the pore walls of the AAO templates, and the wetting lengths along the *z*-axis direction are longer. Similar to the effect of higher annealing temperatures, more irregular edges of the curved PS nanodiscs are generated because more defects on the pore walls are encountered by the front of the wetting polymer melts.

The quantitative relationships of the length of the curved polymer nanodiscs and the annealing conditions are also studied. As mentioned previously, we only measure the wetting lengths along the *z*-axis direction, which are indicated in the graphical illustration and the SEM image (Fig. 5a and b). By measuring the wetting length of the curved PS nanodiscs along the *z*-axis direction, we study the effect of annealing conditions on the wetting behavior of PS nanospheres.

First, the wetting lengths along the *z*-axis direction are measured for the PS (M_w = 78.5 kg mol^{-1}) samples annealed at different temperatures for 25 min. As shown in Fig. 5c, a linear relationship is observed at temperatures from 130–170 °C. The average wetting length of curved PS nanodiscs increases with the annealing temperature because of the decreased viscosities of the polymer melts. When the annealing temperature increases, the viscosities of polymer melts are decreased, and polymer chains exhibit higher mobilities and wet faster the wall surfaces of the AAO nanopores.

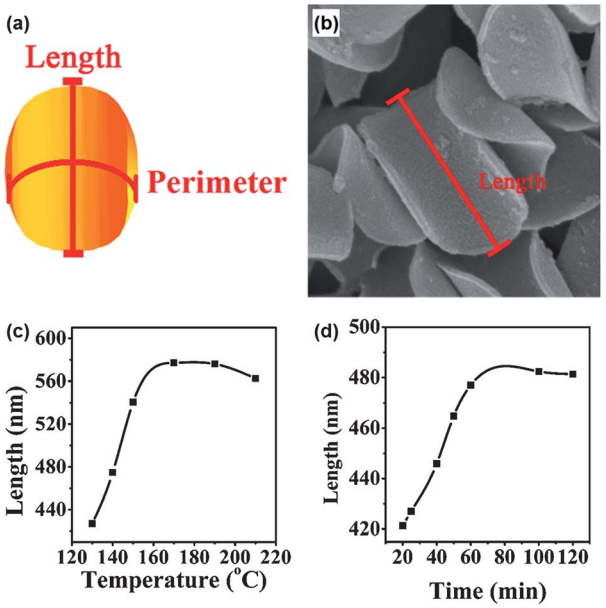

Fig. 5 (a) The illustration of a curved PS nanodisc. The length and perimeter are indicated in the graph. (b) SEM image of a curved PS nanodisc. The length is indicated as a red line in the graph. (c) The plot of the length of curved PS (M_w = 78.5 kg mol^{-1}) nanodiscs *versus* the annealing temperature. The samples are annealed for 25 min. (d) The plot of the length of curved PS (M_w = 78.5 kg mol^{-1}) nanodiscs *versus* the annealing time. The samples are annealed at 130 °C.

As shown in Fig. 5c, the measured values of the wetting lengths reach a plateau region, in which the wetting lengths are ~570 nm, when the annealing temperature is higher than 170 °C. The plateau region is caused by the temperature-dependent viscosities of the polymer melts. The viscosity of a polymer melt is decreased with increased temperatures until a plateau is reached at a critical temperature.[38] Therefore, the viscosities of the polymer melts above a critical temperature are similar, resulting in similar values of the wetting lengths.

We also study the effect of annealing time on the wetting lengths at a fixed annealing temperature. Fig. 5d shows the plot of the length of curved PS (M_w = 78.5 kg mol^{-1}) nanodiscs *versus* the annealing time, while the samples are annealed at 130 °C. The average length increases linearly with the annealing time until a plateau is reached after annealing for 1 h. When the samples are annealed at the same temperatures, the wetting rates of the polymer melts on the pore walls of the AAO templates are the same. The wetting fronts of the polymer melts advance on the wall surfaces and form wetting layers with finite thicknesses that are controlled by the interactions between air, polymer melts, and the alumina walls. Therefore, the wetting length increases with the annealing time until a maximum wetting length is reached. A further increase of the wetting length is not possible because of the volume conservation of the curved PS nanodiscs and the original PS nanospheres. Therefore, the wetting lengths of the polymer nanospheres can be controlled by changing both the annealing temperatures and the annealing times. Changing the annealing temperatures, however, is time-saving and is thus a better way to achieve the desired morphologies and the wetting lengths.

When the polymer nanospheres are formed in the nanopores of the AAO templates by using the non-solvent-assisted template wetting method, the polymer chains are packed loosely. After thermal annealing, a reduction of the volume occupied by the polymer chains is expected. In order to discuss the relationship between the diameters of the original polymer nanospheres and the sizes of the curved polymer nanodiscs, we suppose that the volume is conserved before and after the thermal annealing processes. By assuming that the original polymer nanospheres are all spherical, the volume of the original polymer nanospheres can be described by the following equation:

$$V_s = (4/3)\pi R^3 = (1/6)\pi D^3 \quad (1)$$

where V_s, R, and D represent the volume, the radius, and the diameter of the polymer nanospheres, respectively. Since the surface tension of the polymer melts and the interfacial tension between the polymer melts and the alumina walls are not changing at the same annealing temperature, the polymer melts are expected to form curved discs with similar shapes at long annealing times. By assuming that the thickness over the whole curved polymer nanodisc (H) is constant, the volume of the curved polymer nanodiscs can be described by the following equation:

$$V_p = \pi(L_z/2)^2 H = (1/4)\pi L_z^2 H \quad (2)$$

where V_p is the volume of the curved polymer nanodisc, L_z is the length along the z-axis, and H is the thickness of the curved polymer nanodisc. The volumes before and after thermal annealing processes are assumed to be conserved ($V_s = V_p$), and eqn (1) and (2) can be rewritten as:

$$D^3 = (3/2)L_z^2 H \quad (3)$$

From eqn (3), the wetting lengths (L_z) of the curved polymer nanodiscs increase with the diameters of the original polymer nanospheres. Therefore, the maximum wetting lengths from larger nanospheres are longer.

For most experiments done in this work, polystyrene (PS) is used. To demonstrate the universality of this simple approach, this method is also applied to poly(methyl methacrylate) (PMMA), another common polymer. Similar to the results from PS, curved PMMA nanodiscs can be prepared by using this method, as shown in Fig. S4.† But the morphologies of the curved PMMA nanodiscs are not as well-defined as those of the curved PS nanodiscs. This result might be due to the lower degradation resistance of PMMA to the electron beams in the SEM measurement than that of PS. Still, this result demonstrates that this simple method can be applied to fabricate other types of curved polymer nanodiscs once appropriate wetting conditions are used. Acrylonitrile–butadiene–styrene (ABS) copolymer, a commonly employed polymer material in industry, is also used in this work, and curved ABS nanodiscs are fabricated, as shown in Fig. S5.† Further studies such as electroplating may be applied to these curved nanodiscs to obtain curved metal nanodiscs. In the future, we will apply this method to multicomponent polymer materials such as block copolymers, polymer blends, or polymer composites.

In addition to curved polymer nanodiscs, other morphologies can also be fabricated by this method. For example, helix-like polymer nanostructures and connected polymer nanodiscs are observed after the annealing process, as shown in Fig. 6. Once the polymer nanospheres are fabricated by the non-solvent-assisted template wetting method, most polymer nanospheres in the nanopores of the AAO templates are separated. The average separation distances between the nanospheres are determined by the undulation wavelengths of the polymer solutions during the Rayleigh-instability-type transformation process, as described by Lee *et al.*[29] Some nanospheres, however, are not separated and are stacked on top of each other or merged together, resulting in the formation of helix-like polymer nanostructures or connected polymer nanodiscs. Examples of the merged nanospheres are displayed in the ESI (Fig. S6†).

There are three possible reasons to explain why some nanospheres are stacked or merged together. First, vibrations during the transportation of the nanosphere-containing AAO samples from the desiccator to the oven may cause the nanospheres, which originally adhere to the wall of the nanopores, to stack on top of other nanospheres. Second, the undulation and the separation processes induced by Rayleigh instability may not be completed because of the non-uniform polymer concentrations in the nanopores, resulting in the formation of merged polymer nanospheres. Third, the stacking of the nanospheres might be due to the original defects of the nanopores of the AAO templates.

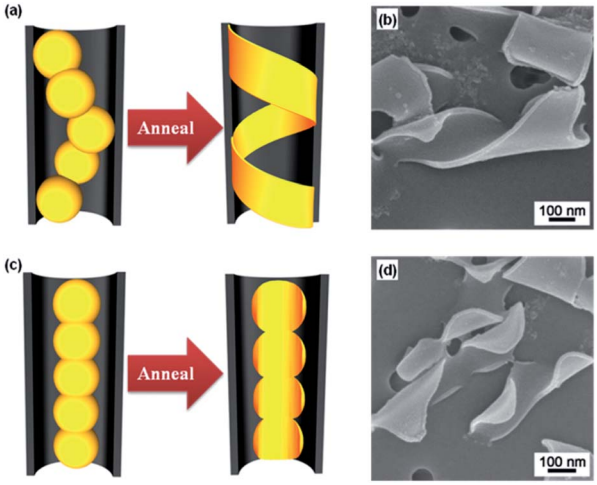

Fig. 6 (a) Graphical illustration of helix-like polymer nanostructures and (b) their corresponding SEM image; (c) graphical illustration of connected polymer nanostructures and (d) their corresponding SEM image. Both samples are obtained by annealing PMMA (M_w = 68.5 kg mol^{-1}) nanospheres at 150 °C for 5 h.

Depending on the arrangements of the stacked or merged nanospheres, a special polymer nanostructure can be formed. If the stacked or merged nanospheres are attached to the pore walls in different orientations, helix-like polymer nanostructures can be formed, as shown in Fig. 6a and b. If the stacked or merged nanospheres are attached to the pore walls on the same sides, connected polymer nanodiscs can be formed, as shown in Fig. 6c and d. These results are observed in both the PS and the PMMA systems. But these kinds of helix-like or connected polymer nanostructures are more often observed in samples annealed at higher temperatures or longer times. With higher temperatures or longer times, the wetting lengths of the polymer nanospheres on the pore walls increase. When the wetting lengths are larger than the distances between two adjacent nanospheres, the helix-like or connected polymer nanostructures can be formed. These kinds of nanostructures can be effectively avoided by using appropriate annealing conditions, and well-defined curved polymer nanodiscs can be produced in a large quantity.

It has been studied that the shape of non-spherical polymer particles is essential for affecting their functionalities and properties. For example, Yunker *et al.* studied that the coffee ring effect, which is commonly seen in polymer spheres, can be eliminated by using ellipsoidal polymer particles.[39] The air–water interfaces are deformed significantly by the anisotropic shape of the particles. Therefore, strong interparticle capillary interactions are produced, leading to the uniform deposition of particles. We have used the spherical polymer nanospheres and curved polymer nanodiscs to study the coffee ring effect. Aqueous solutions containing polymer particles are dropped on

cleaned wafers, followed by a drying process in air. The optical microscopy images are shown in Fig. S7.† Although the coffee ring effect can be observed for both samples, more curved polymer nanodiscs are observed in the center of the dried regions. The results imply that the dynamic behaviors of polymer nanospheres and curved polymer nanodiscs in aqueous solutions are different. Still, more detailed studies need to be performed in the future.

Conclusions

We successfully prepared curved PS nanodiscs by using AAO templates. After post-thermal treatment, the polymer nanospheres in the nanopores transform to curved polymer nanodiscs by wetting on the pore walls of the AAO templates. By changing the experimental conditions such as the annealing temperature and the annealing time, the average lengths of the curved nanodiscs can be controlled. In addition to curved PS nanodiscs, curved PMMA and ABS nanodiscs are also obtained. In the case of stacked polymer nanospheres, helix-like polymer nanostructures are formed after the wetting process. In the future, we will apply this method to other types of polymers including block copolymers, polymer blends, or polymer–metal composites to develop self-assembled anisotropic nanostructures. Compared with isotropic polymer nanospheres, the curved polymer nanodiscs may have interesting dynamic behaviors in aqueous solutions. Therefore, the curved polymer nanodiscs would be useful in applications such as drug delivery and sensing.

Experimental section

Materials

Polystyrene (PS, M_w = 78.5 kg mol^{-1}, PDI = 1.05) and poly(methyl methacrylate) (PMMA, M_w = 68.5 kg mol^{-1}, PDI = 1.25) were purchased from Polymer Source Inc. Acrylonitrile–butadiene–styrene (ABS) copolymers were obtained from Chi Mei Corporation. Anhydrous dimethylformamide (DMF) was obtained from Tedia Company. AAO templates (Anodisc 13) with the average diameters of 0.2 μm were purchased from Whatman. Deionized water was produced by Milli-Q Millipore.

Fabrication of polymer nanospheres in the nanopores of AAO templates

The polymer nanospheres were prepared by the non-solvent-assisted template wetting method.[29] The AAO templates were first dipped into a polymer solution (PS or PMMA 1–5 wt% in DMF) for 10 s. After the templates were taken out from the solution, the surfaces of the templates were first cleaned by delicate task wipers (Kimtech) to remove the solution outside the nanopores, followed by a wiping process on the surface with pure DMF. The AAO templates filled with polymer solutions were then dipped into deionized water for 1 min. Subsequently, the water was poured out, and the samples were dried under vacuum.

Fabrication of curved polymer nanodiscs by wetting polymer nanospheres in the nanopores of AAO templates

The samples with polymer nanospheres in the nanopores of AAO templates were thermally annealed in an oven with temperatures from 120 to 220 °C and annealing times from 10 min to 8 h. After the samples were cooled to room temperature, the samples were dipped in 5 wt% $NaOH_{(aq.)}$ to selectively remove the AAO templates. Finally, the solutions were filtered through membrane filters (0.1 μm, Millipore) and were washed by deionized water.

Structure analysis and characterization

A scanning electron microscope (SEM) (JEOL, JSM-7401F) with an accelerating voltage of 5 kV was used to study the polymer nanostructures. Before SEM measurements, the polymer nanostructures were dried in a desiccator under vacuum and were coated with 4 nm platinum. A transmission electron microscope (TEM) (JEOL, JEM-2100) with an accelerating voltage of 200 kV was also used to investigate the morphologies of the polymer nanostructures.

Notes and references

1 Y. N. Xia, P. D. Yang, Y. G. Sun, Y. Y. Wu, B. Mayers, B. Gates, Y. D. Yin, F. Kim and Y. Q. Yan, *Adv. Mater.*, 2003, **15**, 353–389.
2 T. Kietzke, D. Neher, K. Landfester, R. Montenegro, R. Guntner and U. Scherf, *Nat. Mater.*, 2003, **2**, 408–412.
3 R. H. Baughman, A. A. Zakhidov and W. A. de Heer, *Science*, 2002, **297**, 787–792.
4 L. Vayssieres, *Adv. Mater.*, 2003, **15**, 464–466.
5 A. M. Morales and C. M. Lieber, *Science*, 1998, **279**, 208–211.
6 M. Law, L. E. Greene, J. C. Johnson, R. Saykally and P. D. Yang, *Nat. Mater.*, 2005, **4**, 455–459.
7 G. L. Liu and L. P. Lee, *Appl. Phys. Lett.*, 2005, **87**, 074101.
8 P. V. Kamat, *J. Phys. Chem. B*, 2002, **106**, 7729–7744.
9 M. A. Shannon, P. W. Bohn, M. Elimelech, J. G. Georgiadis, B. J. Marinas and A. M. Mayes, *Nature*, 2008, **452**, 301–310.
10 J. X. Huang, S. Virji, B. H. Weiller and R. B. Kaner, *J. Am. Chem. Soc.*, 2003, **125**, 314–315.
11 Q. A. Pankhurst, J. Connolly, S. K. Jones and J. Dobson, *J. Phys. D: Appl. Phys.*, 2003, **36**, R167–R181.
12 A. K. Geim and K. S. Novoselov, *Nat. Mater.*, 2007, **6**, 183–191.
13 F. Yang, W. H. Liu, X. W. Wang, J. Zheng, R. Y. Shi, H. Zhao and H. Q. Yang, *ACS Appl. Mater. Interfaces*, 2012, **4**, 3852–3859.
14 C. L. Lee, C. M. Syu, C. H. Huang, H. P. Chiou, Y. J. Chao and C. C. Yang, *Appl. Catal., B*, 2013, **132**, 229–236.
15 L. Hyun Woo, O. Jin Young, L. Tae Il, J. Woo Soon, Y. Young Bum, C. Soo Sang, P. Jee Ho, M. Jae Min, S. Kie Moon and B. Hong Koo, *Appl. Phys. Lett.*, 2013, **102**, 193903.
16 M. M. Liu and W. Chen, *Biosens. Bioelectron.*, 2013, **46**, 68–73.
17 C. C. Ho, A. Keller, J. A. Odell and R. H. Ottewill, *Colloid Polym. Sci.*, 1993, **271**, 469–479.

18 J. A. Champion, Y. K. Katare and S. Mitragotri, *Proc. Natl. Acad. Sci. USA*, 2007, **104**, 11901–11904.
19 S. Hongrok and K. Chongyoup, *Colloid Polym. Sci.*, 2012, **290**, 1309–1315.
20 B. Liu and D. Y. Wang, *Langmuir*, 2012, **28**, 6436–6440.
21 N. Haberkorn, M. C. Lechmann, B. H. Sohn, K. Char, J. S. Gutmann and P. Theato, *Macromol. Rapid Commun.*, 2009, **30**, 1146–1166.
22 C. R. Martin, *Science*, 1994, **266**, 1961–1966.
23 J. Martin, J. Maiz, J. Sacristan and C. Mijangos, *Polymer*, 2012, **53**, 1149–1166.
24 M. Steinhart, R. B. Wehrspohn, U. Gosele and J. H. Wendorff, *Angew. Chem., Int. Ed.*, 2004, **43**, 1334–1344.
25 M. Steinhart, J. H. Wendorff, A. Greiner, R. B. Wehrspohn, K. Nielsch, J. Schilling, J. Choi and U. Gosele, *Science*, 2002, **296**, 1997.
26 P. Dobriyal, H. Q. Xiang, M. Kazuyuki, J. T. Chen, H. Jinnai and T. P. Russell, *Macromolecules*, 2009, **42**, 9082–9088.
27 J. Maiz, J. Martin and C. Mijangos, *Langmuir*, 2012, **28**, 12296–12303.
28 J. T. Chen, C. W. Lee, M. H. Chi and I. C. Yao, *Macromol. Rapid Commun.*, 2013, **34**, 348–354.
29 C. W. Lee, T. H. Wei, C. W. Chang and J. T. Chen, *Macromol. Rapid Commun.*, 2012, **33**, 1381–1387.
30 S. Schlitt, A. Greiner and J. H. Wendorff, *Macromolecules*, 2008, **41**, 3228–3234.
31 X. D. Feng and Z. X. Jin, *Macromolecules*, 2009, **42**, 569–572.
32 M. F. Zhang, P. Dobriyal, J. T. Chen, T. P. Russell, J. Olmo and A. Merry, *Nano Lett.*, 2006, **6**, 1075–1079.
33 A. M. M. Jani, D. Losic and N. H. Voelcker, *Prog. Mater. Sci.*, 2013, **58**, 636–704.
34 H. Masuda and K. Fukuda, *Science*, 1995, **268**, 1466–1468.
35 A. P. Li, F. Muller, A. Birner, K. Nielsch and U. Gosele, *J. Appl. Phys.*, 1998, **84**, 6023–6026.
36 F. A. Nichols and W. W. Mullins, *Trans. Metall. Soc. AIME*, 1965, **233**, 1840–1848.
37 X. D. Feng, S. L. Mei and Z. X. Jin, *Langmuir*, 2011, **27**, 14240–14247.
38 H. Kobayashi, H. Takahashi and Y. Hiki, *Mater. Sci. Eng., A*, 2006, **442**, 263–267.
39 P. J. Yunker, T. Still, M. A. Lohr and A. G. Yodh, *Nature*, 2011, **476**, 308–311.

